

Plane correlations and hydrodynamic simulations of heavy ion collisions

D. Teaney*

*Department of Physics & Astronomy,
Stony Brook University, Stony Brook, NY 11794, USA*

L. Yan

CNRS, Institut de Physique Théorique de Saclay, F-91191 Gif-sur-Yvette, France †

(Dated: May 17, 2022)

Abstract

We use a nonlinear response formalism to describe the event plane correlations measured by the ATLAS collaboration. With one exception ($\langle \cos(2\Psi_2 - 6\Psi_3 + 4\Psi_4) \rangle$), the event plane correlations are qualitatively reproduced by considering the linear and quadratic response to the lowest cumulants. For the lowest harmonics such as $\langle \cos(2\Psi_2 + 3\Psi_3 - 5\Psi_5) \rangle$, the correlations are quantitatively reproduced, even when the naive Glauber model prediction has the wrong sign relative to experiment. The quantitative agreement for the higher plane correlations (especially those involving Ψ_6) is not as good. The centrality dependence of the correlations is naturally explained as an average of the linear and quadratic response.

* derek.teaney@stonybrook.edu

† li.yan@cea.fr

I. INTRODUCTION

The collective expansion of the deconfined fireball created in high energy heavy-ion collisions maps the initial state of the Quark-Gluon Plasma (QGP) to the final state particle spectrum. The measured correlations in this spectrum can clarify the initial conditions and subsequent expansion dynamics of the QGP [1–3].

On an event-event basis the azimuthal distribution of produced particles can be decomposed into a Fourier series

$$\frac{dN}{d\phi_{\mathbf{p}}} = \frac{N}{2\pi} \left(1 + 2 \sum_{n=1}^{\infty} v_n \cos(n\phi_{\mathbf{p}} - n\Psi_n) \right), \quad (1.1)$$

and the measured two particle correlation function determines the root mean square of these harmonics, $\sqrt{\langle v_n^2 \rangle}$. The magnitude of these harmonics is reasonably reproduced by event-by-event viscous hydrodynamics provided the shear viscosity is not too large [1]. The correlations between the harmonics can provide new tests of the hydrodynamic description, constrain the simulation parameters, and provide an estimate of the uncertainties in the computation. In this work we will describe the correlations between the observed event plane angles Ψ_n in order to clarify the expansion dynamics, and ultimately to determine the shear viscosity of the QGP with credible systematic error bars.

Clearly, an important input to the hydrodynamic simulations is the distribution of energy density in the transverse plane, which is usually estimated from the known probability distribution of nucleons in the incoming nuclei. There is reasonable evidence, both experimental [4] and theoretical [5], that v_2 and v_3 are to a good approximation linearly proportional to the corresponding angular fluctuations in the transverse energy density. However, event-by-event hydrodynamic simulations have shown that the higher harmonics, v_4 and v_5 , reflect both the response to corresponding angular harmonics in the initial state, and the non-linear hydrodynamic response which mixes lower order harmonics [5, 6]. For example, the 5-th flow harmonic, v_5 , is determined in part by the medium response to the 5-th harmonic of the initial energy density distribution, and in part by the non-linear mixing between v_2 and v_3 . Such mode-mixing is especially important at high p_T where the non-linearities of the phase-space distribution play an important role [7]. Motivated by these simulation results, and especially the simulation analysis of Ref. [6], we developed a non-linear response formalism to describe the mixing between modes of different order, and we investigated how the response coefficients depend on centrality, shear viscosity, and transverse momentum [8].

These theoretical calculations preceded the corresponding experimental studies by the ATLAS [9] and ALICE collaborations [10], which qualitatively confirmed the mode mixing picture by measuring significant correlations between the event-plane angles of different orders¹, *e.g.* between Ψ_2, Ψ_3 , and Ψ_5 . Event-by-event hydrodynamics [12] and AMPT calculations [13] largely reproduce the structure of these correlations. The goal of this paper is to compare the response formalism outlined in our previous work to the event-plane correlations measured by the ATLAS collaboration [8].

As discussed more technically in Section II B we will use a non-linear response formalism to describe the observed event plane correlations, rather than event-by-event hydrodynamics.

¹ The ATLAS measurement did not precisely measure Ψ_n [11]. Ultimately, this important first measurement will need to be redone, weighting the event averages with the Q vector to provide an unambiguous quantity which can be compared to fairly compared to simulations. See below for further discussion.

In practice, this means that we decompose the initial state into an average event plus small fluctuations, which are systematically analyzed with cumulants. The linear and quadratic response to each cumulant is found by perturbing the average background, and finally the observed plane correlations are found by weighting the response functions with the spectrum of fluctuations. Thus, the response formulation provide a transparent link between the initial state and the final state, which contains *only* the linear and quadratic response through a specified order in the cumulant expansion. As we will see, this approach reproduces a lot of the observed event plane correlations, suggesting that most of the microscopic details of the initial state (beyond the lowest cumulants) are irrelevant. Ideally, a limited number of initial state parameters can be extracted from experiment, and compared to available theoretical frameworks such as the Color Glass Condensate to demonstrate the consistency and uniqueness of the approach. There are indications that the spectrum of fluctuations from the Color Glass Condensate is consistent with the observed harmonics [14], but the uniqueness of this approach is not obvious.

A review of the non-linear flow response formalism will be given in Section II. This has several ingredients. First, the spectrum of initial fluctuations in various Glauber type models is described in Section II A, and this spectrum is analyzed with the cumulant and moment expansions. Then, we describe how the response coefficients are calculated, and how these coefficients determine the plane correlations in Section II B and Section II C. Finally, we compare the response formalism to the ATLAS data in Section III and discuss the results.

Throughout the paper Φ_n will denote participant plane angle based on the *cumulants* rather than moments. (The correlations in the Glauber model between the cumulant angles Φ_n are markedly different from the correlations found using the analogous moment based angles – see Section II A.) Ψ_n denotes the event plane angle extracted from the final state momentum spectra.

II. REVIEW OF NONLINEAR FLOW RESPONSE FORMALISM

A. Characterizing the initial state with cumulants

As discussed in the introduction, an important input to the hydrodynamic calculations is the spectrum of initial fluctuations. This spectrum is traditionally [4] quantified with the participant plane anisotropy based on moments²

$$\varepsilon_n e^{in\Phi_n} \equiv -\frac{\langle r^n e^{in\phi_r} \rangle}{\langle r^n \rangle} \quad (\text{Not used}). \quad (2.1)$$

Here the brackets $\langle \dots \rangle$ denote an average over the participating nucleons of a single event, while $re^{i\phi_r} = x + iy$ notates the transverse coordinates of the participants. It is convenient to use a complex notation $z \equiv x + iy$ so that $\varepsilon_n e^{in\Phi_n} = -\langle z^n \rangle / \langle r^n \rangle$. As emphasized in our previous work, it is often useful to characterize the fluctuations with cumulants rather than moments. The cumulants subtract off the lower order correlation functions of z to describe

² In this formula we are using a moment based definition of ε_n and Φ_n . For most of the text we will use a cumulant based definition.

the irreducible correlations

$$\varepsilon_n e^{in\Phi_n} \equiv -\frac{1}{r^n} [\langle z^n \rangle - \text{subtractions}] . \quad (2.2)$$

For example, the fourth order cumulant is

$$\varepsilon_4 e^{i4\Phi_4} \equiv -\frac{1}{\langle r^4 \rangle} [\langle z^4 \rangle - 3 \langle z^2 \rangle^2] , \quad (2.3)$$

where the factor of three arises because there are three ways to pair four objects. Here and below we have assumed that we are working in the center of mass coordinate system where $\langle z \rangle = 0$. The usefulness of cumulants can be understood by considering a Gaussian distribution,

$$\rho(x, y) \propto e^{-\frac{x^2}{2\langle x^2 \rangle} - \frac{y^2}{2\langle y^2 \rangle}} , \quad (2.4)$$

whose fourth order moment anisotropy $\langle z^4 \rangle$ is non-zero, and is trivially correlated with the eccentricity, $\langle z^2 \rangle$. The fourth order cumulant takes out these trivial correlations, and for a Gaussian distribution we have $\varepsilon_4 \propto \langle z^4 \rangle - 3 \langle z^2 \rangle^2 = 0$.

The azimuthal anisotropies through ε_6 are

$$\mathcal{E}_2 \equiv \varepsilon_2 e^{i2\Phi_2} \equiv -\frac{\langle z^2 \rangle}{\langle r^2 \rangle} , \quad (2.5)$$

$$\mathcal{E}_3 \equiv \varepsilon_3 e^{i3\Phi_3} \equiv -\frac{\langle z^3 \rangle}{\langle r^3 \rangle} , \quad (2.6)$$

$$\mathcal{E}_4 \equiv \varepsilon_4 e^{i4\Phi_4} \equiv -\frac{1}{\langle r^4 \rangle} [\langle z^4 \rangle - 3 \langle z^2 \rangle^2] , \quad (2.7)$$

$$\mathcal{E}_5 \equiv \varepsilon_5 e^{i5\Phi_5} \equiv -\frac{1}{\langle r^5 \rangle} [\langle z^5 \rangle - 10 \langle z^2 \rangle \langle z^3 \rangle] , \quad (2.8)$$

$$\mathcal{E}_6 \equiv \varepsilon_6 e^{i6\Phi_6} \equiv -\frac{1}{\langle r^6 \rangle} [\langle z^6 \rangle - 15 \langle z^4 \rangle \langle z^2 \rangle - 10 \langle z^3 \rangle^2 + 30 \langle z^2 \rangle^3] , \quad (2.9)$$

where $\mathcal{E}_n = \varepsilon_n e^{in\Phi_n}$ denotes the eccentricity and its phase. The ε_1 which drives v_1 is a special case, and is given by

$$\mathcal{E}_1 = \varepsilon_1 e^{i\Phi_1} \equiv -\frac{1}{\langle r^3 \rangle} \langle z^2 z^* \rangle . \quad (2.10)$$

Given an initial state Glauber model for the distribution of nucleons such as Glissando [15] or the Phobos Monte Carlo Glauber model [16] one can calculate the correlations between the angles Φ_n . Fig. 1 and Fig. 2 show such a calculation from the Phobos Monte-Carlo model. Here and below the double brackets $\langle\langle \dots \rangle\rangle$ indicate an average over events, while the single brackets $\langle \dots \rangle$ denote an average over one event. In the Phobos Glauber the participant centers are used to define the averages in eq. (2.5), while in the Glissando model a slightly different prescription is used, which is based on the wounding profile of the nucleon [15].

It is interesting to compare the correlations between the cumulant and moment based angles. For example, the $\langle\langle \cos 4(\Phi_4 - \Phi_2) \rangle\rangle$ correlation is strongly negative with the moment based definitions, while the corresponding correlations with cumulant angles are positive. In the moment definition the Φ_4, Φ_2 correlation arises because the fourth order eccentricity \mathcal{E}_4

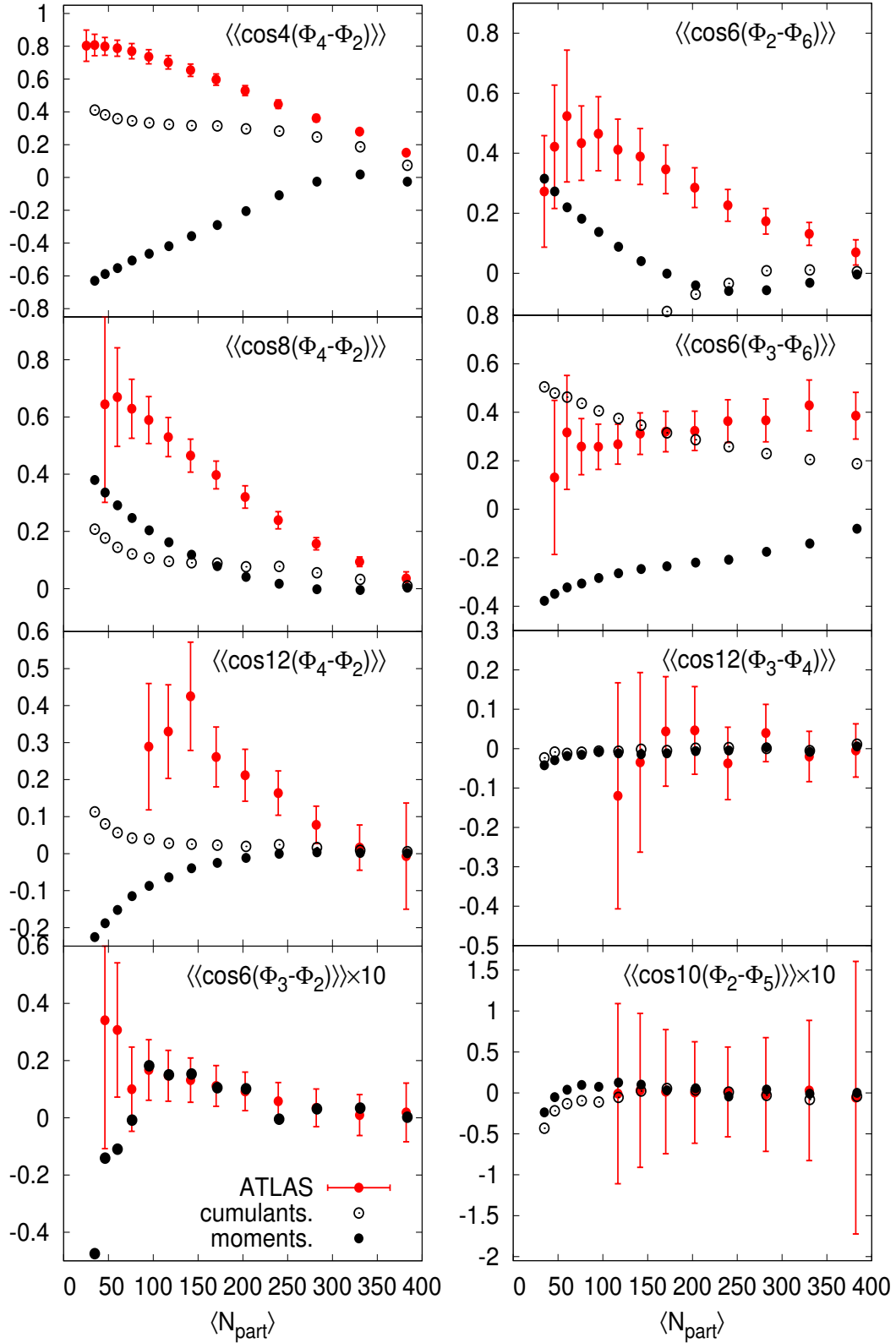


FIG. 1. Participant 2-plane correlations from Phobos Monte Carlo Glauber model [16] as measured by the cumulant and moment expansions. The measured event plane correlations [9] are presented for reference and as a point of contact, and are not supposed to be directly compared to the Glauber model results.

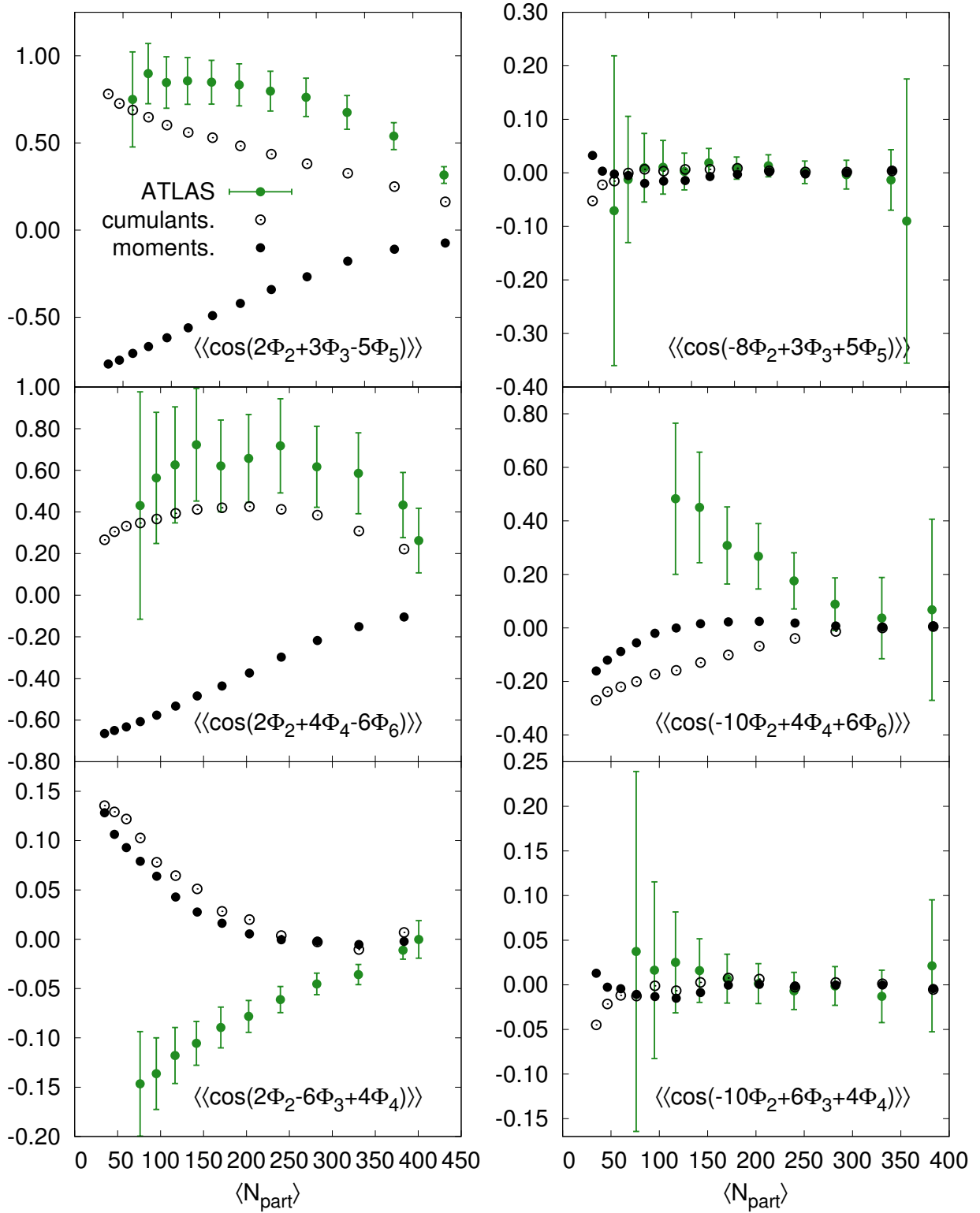


FIG. 2. Participant 3-plane correlations from Phobos Monte Carlo Glauber model [16] as measured by the cumulant and moment expansions. The measured event plane correlations [9] are presented for reference and as a point of contact, and are not supposed to be directly compared to the Glauber model results.

is trivially correlated with the second order eccentricity \mathcal{E}_2 through the average geometry. These trivial geometric correlations are removed with the cumulant definition, and the residual correlation is positive. The correlation between Ψ_4 and Ψ_2 seen in the data is positive, but does not seem to be directly related to the participant plane correlation between Φ_4 and Φ_2 . The interpretation of the data is described in Section III.

B. Formulation of flow response

The harmonic flow v_n and the corresponding flow angle Ψ_n are defined by the Fourier decomposition of the final state particle spectrum,

$$\frac{dN}{d\phi_p} = \frac{N}{2\pi} \left[1 + \sum_n (v_n e^{-in(\phi_p - \Psi_n)} + c.c.) \right]. \quad (2.11)$$

Here we use a complex expression, with *c.c.* standing for complex conjugate. For simplicity, we also define a complex flow coefficient which takes into account the flow and its angle simultaneously,

$$V_n \equiv v_n e^{in\Psi_n}. \quad (2.12)$$

Following the same strategy and notation as in our previous work [8], the magnitude of the flow and its corresponding angle is given by the response formula

$$V_n = \left(\frac{w_n}{\varepsilon_n} \right) \mathcal{E}_n + \sum_{\text{quadratic}} \left(\frac{w_{n(pq)}}{\varepsilon_p \varepsilon_q} \right) \mathcal{E}_p \mathcal{E}_q + \dots \quad (2.13)$$

Here w_n is the n -th linear response coefficient to a given \mathcal{E}_n , and $w_{n(pq)}$ are the n -th quadratic response coefficients. The ellipses in eq. (2.13) stand for higher order nonlinear contributions which are generally neglected in this work. The only exception to this rule is for V_6 where we included the contribution from \mathcal{E}_2^3 . Even in this case, the \mathcal{E}_2^3 contribution was found to be numerically small compared to the quadratic $\mathcal{E}_2 \mathcal{E}_4$ and the \mathcal{E}_3^2 results. The current calculation uses the following minimal set of response coefficients

$$w_1 \dots w_6 \quad w_{1(32)}, w_{3(21)}, w_{4(22)}, w_{5(23)}, w_{6(24)}, w_{6(33)}, w_{6(222)}. \quad (2.14)$$

We found that additional non-linear terms such as $w_{2(31)}$, $w_{4(13)}$, and $w_{5(14)}$ were not numerically important for the current set of correlations. Thus, we reverted the code to the minimal set of response coefficients listed in eq. (2.14). The effects of including additional (radial) modes in the linear response was studied in [17, 18]. While a complete analysis will be presented in future work, a preliminary investigation shows that these (radial) contributions are small for the inclusive correlations studied here.

The form of eq. (2.13) indicates the dependence of the n -th order harmonic flow and its angle on the linear response coefficient w_n and the quadratic response coefficients $w_{n(pq)}$. These response coefficients are calculated by perturbing the (smooth) background geometry and determining the resulting flow. The details of this procedure have been given in our previous work [8], and here we will simply review the most important features.

Linear and nonlinear flow response coefficients are obtained from “single-shot” 2+1D hydrodynamic simulations. In this approach the average geometry for a given centrality

class is modeled with a cylindrically symmetric Gaussian, *i.e.* the initial entropy density in the event at Bjorken time τ_o is

$$s(x, y, \tau_o) = \frac{C_s}{\tau_o \pi R^2} e^{-r^2/R^2}. \quad (2.15)$$

The rms radius of the Gaussian is adjusted to match the rms radius of a smooth (or averaged) Glauber model for a given centrality. The overall constant of the Gaussian is adjusted as a function of centrality to reproduce the measured dN_{ch}/dy at the LHC [19]. The response coefficients are calculated by perturbing this radially symmetric Gaussian by small deformations; running the perturbed Gaussian through the hydro tool chain; and finally calculating w_n or $w_{n(pq)}$. For example, for we calculate w_5/ϵ_5 by deforming the Gaussian by a tiny ϵ_5 and calculating v_5 . Similarly we calculate $w_{5(23)}/(\epsilon_2\epsilon_3)$ by deforming the Gaussian by ϵ_2 and by ϵ_3 and calculating v_5 , which is proportional to $\epsilon_2\epsilon_3$. To summarize, all of the response coefficients and their dependence on centrality are obtained by simulating slightly deformed cylindrically symmetric Gaussian initial conditions.

We have implemented 2nd order BRSSS hydrodynamics, taking the necessary second order transport coefficients from the AdS/CFT results. The numerical scheme (but not the code) is similar to the scheme developed in Ref. [20]. The shear viscosity to entropy ratio η/s is constant throughout the whole evolution, and is set to the canonical value of $1/4\pi$. We use an equation of state that parametrizes the lattice results [21], which was used previously by Romatschke and Luzum [22]. Finally, we use a constant freeze-out temperature $T_{\text{fo}} = 150$ MeV, and adopt the widely used quadratic ansatz for the first viscous correction to the freeze-out distribution function [23].

C. Formulation of plane correlations

The plane correlations are measured by event-plane method [9], and a multi-particle correlation method [10, 24]. We will focus on the event plane method which was used by the ATLAS collaboration. The details of this method were clarified by Luzum and Ollitrault who showed that if the event plane method is used, the quantity that is measured depends on the reaction plane resolution of the detector [11].

We are interested in describing the correlations involving two and three event plane angles. For definiteness we will present formulas for a specific correlation, $\langle\langle \cos(4\Psi_4 - 2(2\Psi_2)) \rangle\rangle$, which can be easily generalized to other harmonics. (To aid the reader we have written $4\Psi_2 = 2(2\Psi_2)$ to expose the general pattern.) The 4-2 plane correlation is related to V_4 and V_2 through

$$\langle\langle \cos(4\Psi_4 - 2(2\Psi_2)) \rangle\rangle = \left\langle\left\langle \frac{\text{Re}(V_4 V_2^{*2})}{\sqrt{(V_4 V_4^*)(V_2 V_2^*)^2}} \right\rangle\right\rangle = \left\langle\left\langle \frac{w_4 \cos 4(\Phi_4 - \Phi_2) + w_{4(22)}}{|w_4 e^{-i4\Phi_4} + w_{4(22)} e^{-i4\Phi_2}|} \right\rangle\right\rangle. \quad (2.16)$$

Thus, both the linear and nonlinear response coefficients enter this formula for the event plane correlation.

The ATLAS collaboration quantified the event plane correlations by measuring related correlations between the experimental planes, $\hat{\Psi}_n$, as determined by the Q_n -vectors, $\hat{Q}_n = |Q_n| e^{-in\hat{\Psi}_n}$ [9]. Further investigation showed that the measured quantity can not be directly

interpreted as an event plane correlation in the form of eq. (2.16). The measured correlation equals eq. (2.16) when the experimental event plane resolution approaches unity,

$$\langle \cos(4\hat{\Psi}_2 - 2(2\hat{\Psi}_2)) \rangle \{EP\} \simeq \left\langle \left\langle \frac{\text{Re}(V_4 V_2^{*2})}{\sqrt{(V_4 V_4^*)(V_2 V_2^*)^2}} \right\rangle \right\rangle \quad (\text{high resolution limit}). \quad (2.17)$$

Here we have notated the experimental quantity with $\{EP\}$ [9], and refer to Ref. [11] where the precise definition is carefully examined. The notation for the experimental quantity is somewhat misleading since the experimental definition does not actually correspond to the average of a cosine, and can be greater than one. In the limit of low event plane resolution, the measured quantity equals

$$\langle \cos(4\hat{\Psi}_2 - 2(2\hat{\Psi}_2)) \rangle \{EP\} \simeq \frac{\langle \langle \text{Re}(V_4 V_2^{*2}) \rangle \rangle}{\sqrt{\langle \langle V_4 V_4^* \rangle \rangle \langle \langle (V_2 V_2^*)^2 \rangle \rangle}} \quad (\text{low resolution limit}). \quad (2.18)$$

Clearly eq. (2.18) differs from eq. (2.17) by how the events are weighted. The event plane measurements by the ATLAS collaboration (such as $\langle \cos(4\hat{\Psi}_2 - 2(2\hat{\Psi}_2)) \rangle \{EP\}$) interpolate between the high and low resolution limits depending on the reaction plane resolution.

As the experimental resolution depends on the harmonic number, the detector acceptance, and centrality, we will compute both the high and low resolution limits and compare both curves to the experimental data. In the future, such ambiguities in the measurement definition can be avoided by measuring

$$\frac{\langle v_4 v_2^2 \cos(4\hat{\Psi}_2 - 2(2\hat{\Psi}_2)) \rangle}{\sqrt{\langle v_2^2 \rangle^2 \langle v_4^2 \rangle}} = \frac{\langle \langle \text{Re}(V_4 V_2^{*2}) \rangle \rangle}{\sqrt{\langle \langle V_4 V_4^* \rangle \rangle \langle \langle (V_2 V_2^*)^2 \rangle \rangle^2}}, \quad (2.19)$$

as originally suggested in [25], and more recently in [11]. Such angular of correlations have already been measured by the ALICE collaboration [10], but we will not address this preliminary data here. Certainly eq. (2.19) is the most natural from the perspective of the response formalism developed in this work.

Finally, we give one additional example, $-8\Psi_2 + 3\Psi_3 + 5\Psi_5$ of how a three plane correlation function is calculated in the high and low resolution limits:

$$\langle \cos(-4(2\hat{\Psi}_2) + 3\hat{\Psi}_3 + 5\hat{\Psi}_5) \rangle \{EP\} \simeq \left\langle \left\langle \frac{\text{Re}(V_2^{*4} V_3 V_5)}{\sqrt{(V_2 V_2^*)^4 (V_5 V_5^*) (V_3 V_3^*)}} \right\rangle \right\rangle \quad (\text{high resolution}), \quad (2.20)$$

$$\langle \cos(-4(2\hat{\Psi}_2) + 3\hat{\Psi}_3 + 5\hat{\Psi}_5) \rangle \{EP\} \simeq \frac{\langle \langle \text{Re}(V_2^{*4} V_3 V_5) \rangle \rangle}{\sqrt{\langle \langle (V_2 V_2^*)^4 \rangle \rangle \langle \langle V_3 V_3^* \rangle \rangle \langle \langle V_5 V_5^* \rangle \rangle}} \quad (\text{low resolution}). \quad (2.21)$$

In the future the quantity which is most easily compared to theoretical calculations is

$$\frac{\langle v_2^4 v_3 v_5 \cos(-4(2\hat{\Psi}_2) + 3\hat{\Psi}_3 - 5\hat{\Psi}_5) \rangle}{\sqrt{\langle v_2^2 \rangle^4 \langle v_3^2 \rangle \langle v_5^2 \rangle}} = \frac{\langle \langle \text{Re}(V_2^{*4} V_3 V_5) \rangle \rangle}{\sqrt{\langle \langle (V_2 V_2^*)^4 \rangle \rangle \langle \langle V_3 V_3^* \rangle \rangle \langle \langle V_5 V_5^* \rangle \rangle}}. \quad (2.22)$$

III. DISCUSSIONS AND CONCLUSIONS

Figs. 3 and 4 show a comparison of the measured two and three plane correlation functions with the response formalism in the high and low resolution limits using the PHOBOS Glauber. To test the sensitivity to the Glauber model in the high resolution limit we compare two widely used monte-carlos – the PHOBOS Monte Carlo Glauber [16] and Glissando [15]. In Figs. 5 and 6, the predictions of viscous hydrodynamics based on these two initial state models are shown by the blue and green lines, respectively. The two Glauber models give similar results, although the correlations from Glissando are somewhat stronger.

For the highest harmonics (such as v_6), viscous corrections in peripheral collisions can become too large to be trusted. In this regime the linear and non-linear response coefficients can become negative as a result of the first viscous correction to the distribution function [8]. Second order corrections to the viscous distribution are positive [23], suggesting that such negative response coefficients are artificial. Indeed, kinetic theory simulations have positive response coefficients for all values of the Knudsen parameter [28]. To understand when viscous corrections to the response coefficients are out of control, we have performed two simulations. In the first case (un-cut), we blindly allow the response coefficients to become negative. In the second case (cut), we set these coefficients to zero (as a function of centrality) when they turn negative. In Figs. 5 and 6 we show the correlation results of the un-cut (solid) and cut (dashed) response coefficients. As seen in these figures, the ambiguity is noticeable only for peripheral collisions, and for correlations involving the highest harmonic, Ψ_6 . Examining the $\langle\langle \cos 6(\Psi_6 - \Psi_3) \rangle\rangle$ correlation, we see that the negative dive in peripheral collisions is an artifact of out-of-control viscous corrections. A similar negative dive is seen in event-by-event hydro simulations [12].

Inspecting these correlations, we make the following observations. First, many of the most important correlation functions are reasonably reproduced, at least if the high resolution limit is used. The agreement with the low resolution limit is not as good. The ambiguities in the measurement can be avoided by taking definite moments as in eq. (2.19) [25]. Examining the definitions of the high and low resolution limits (Eqs. 2.17 and 2.18), we see that the difference between the two measurements can be best quantified by measuring the probability distribution $P(v_n)$ [26], or the moments of this distribution [27], *e.g.* for v_2

$$(v_2\{2\})^2 \equiv \langle v_2^2 \rangle \quad \text{and} \quad (v_2\{4\})^4 \equiv -[\langle v_2^4 \rangle - 2\langle v_2^2 \rangle] . \quad (3.1)$$

It is then a separate and important question whether the response formalism outlined here can reproduce these probability distributions. This will be addressed in future work.

There are a few correlations which are seemingly not well reproduced even in the high resolution limit. First, one could hope for better agreement with the correlations involving Ψ_6 such as $\cos(6\Psi_3 - 6\Psi_6)$ and $\cos(6\Psi_2 - 6\Psi_6)$. v_6 is a relatively high harmonic, and viscous corrections are not in perfect control in peripheral collisions [23]. This is clearly evident in Fig. 5 which estimates the contributions of higher order viscous corrections to the distribution function (see above). For the Ψ_6 -correlations (and no others), these corrections are large in peripheral collisions.

The most troubling correlation function, which is not qualitatively reproduced by the response formulation, is $\cos(2\Psi_2 - 6\Psi_3 + 4\Psi_4)$. It is possible that that this discrepancy stems from an underestimate of the mixing of v_1 with other modes, which naturally mixes

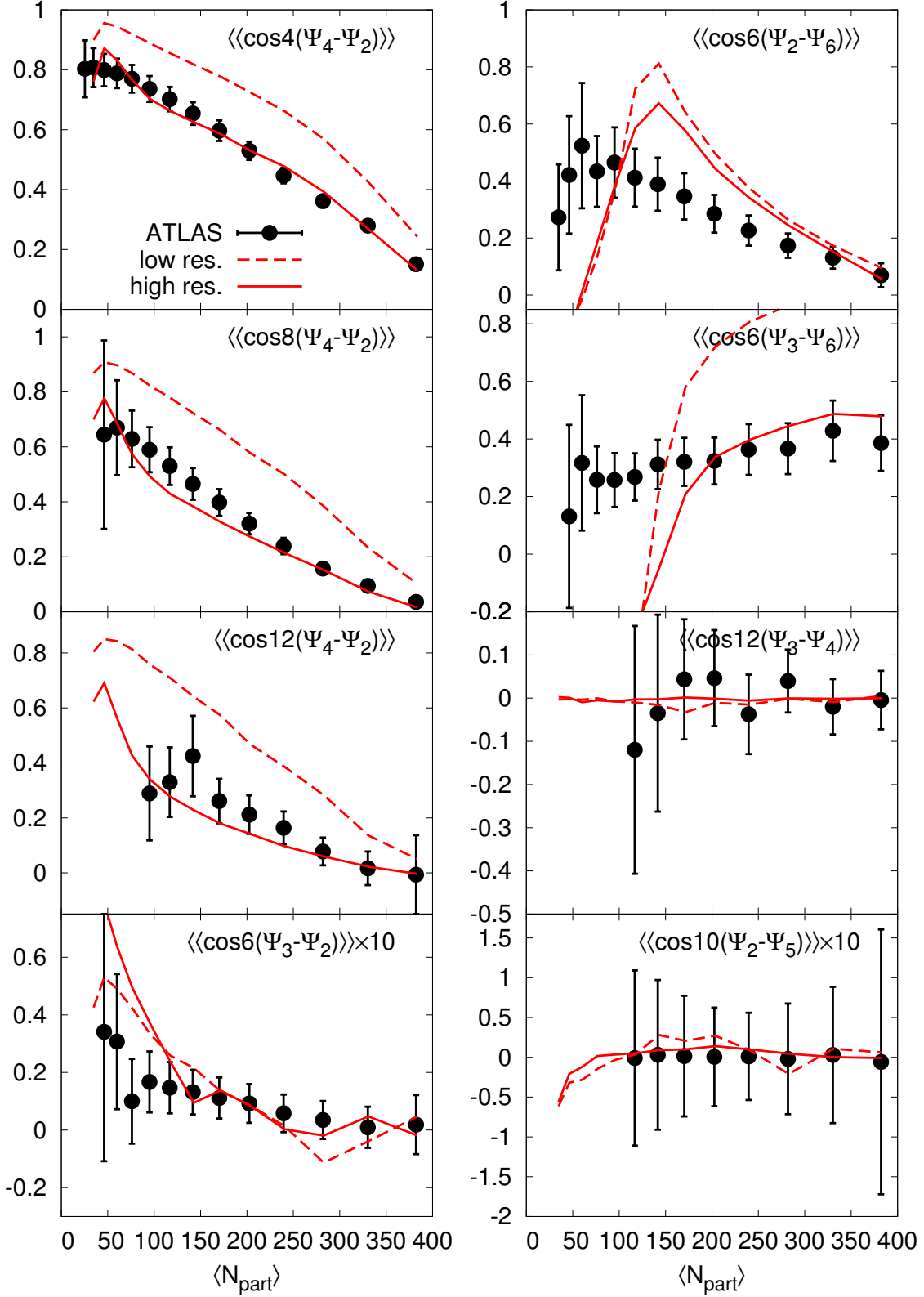


FIG. 3. Two plane correlations using the non-linear response formalism. Here $\eta/s = 1/4\pi$ for PHOBOS Monte-Carlo Glauber initial conditions. The data are from the ATLAS collaboration [9]. The solid lines indicate the high resolution limit, eq. (2.17), while the dashed lines indicate the low resolution limit, eq. (2.18).

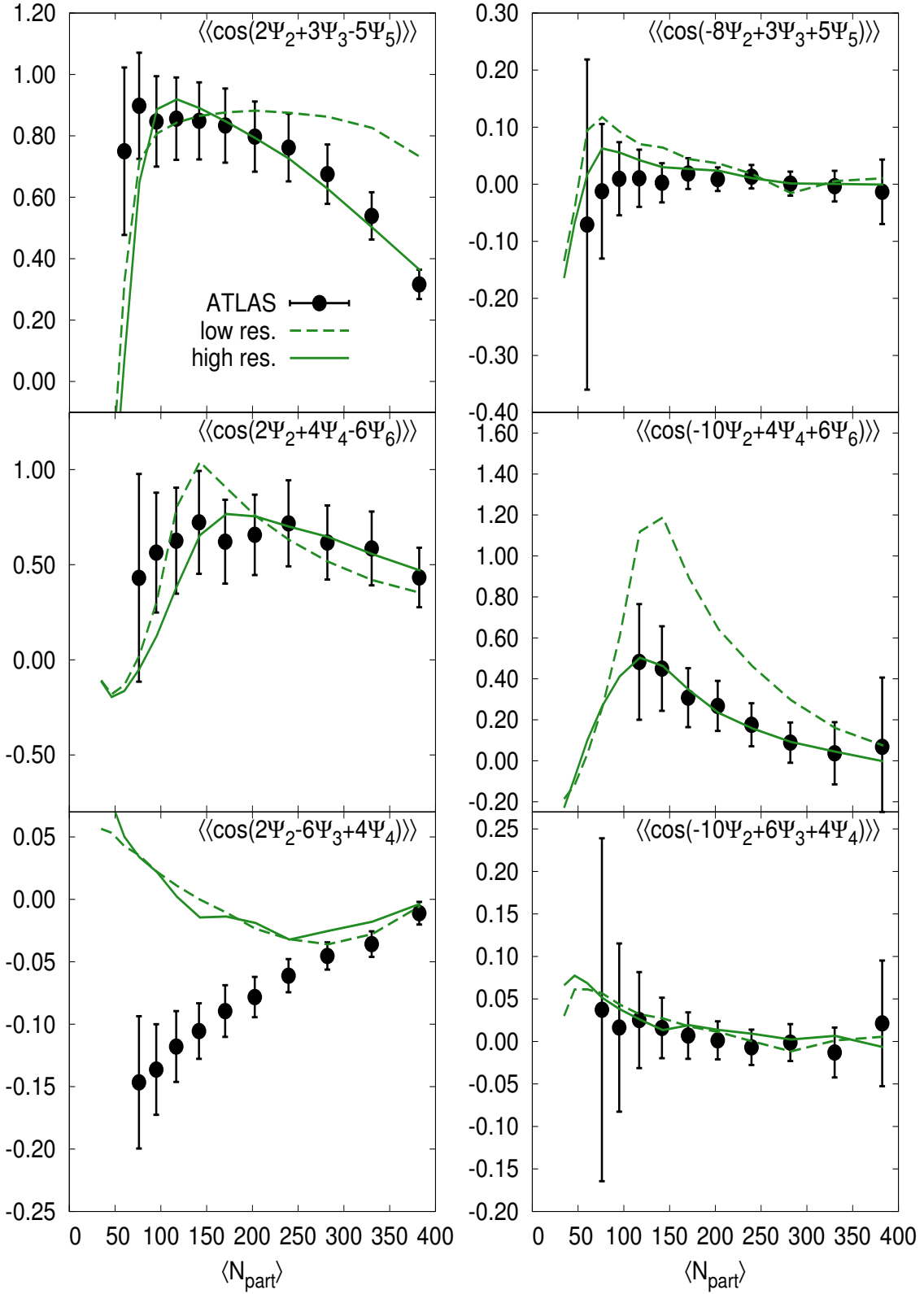


FIG. 4. Three plane correlations using the non-linear response formalism. Here $\eta/s = 1/4\pi$ for PHOBOS Monte-Carlo Glauber initial conditions. The data are from the ATLAS collaboration [9]. The solid lines indicate the high resolution limit, eq. (2.17), while the dashed lines indicate the low resolution limit, eq. (2.18).

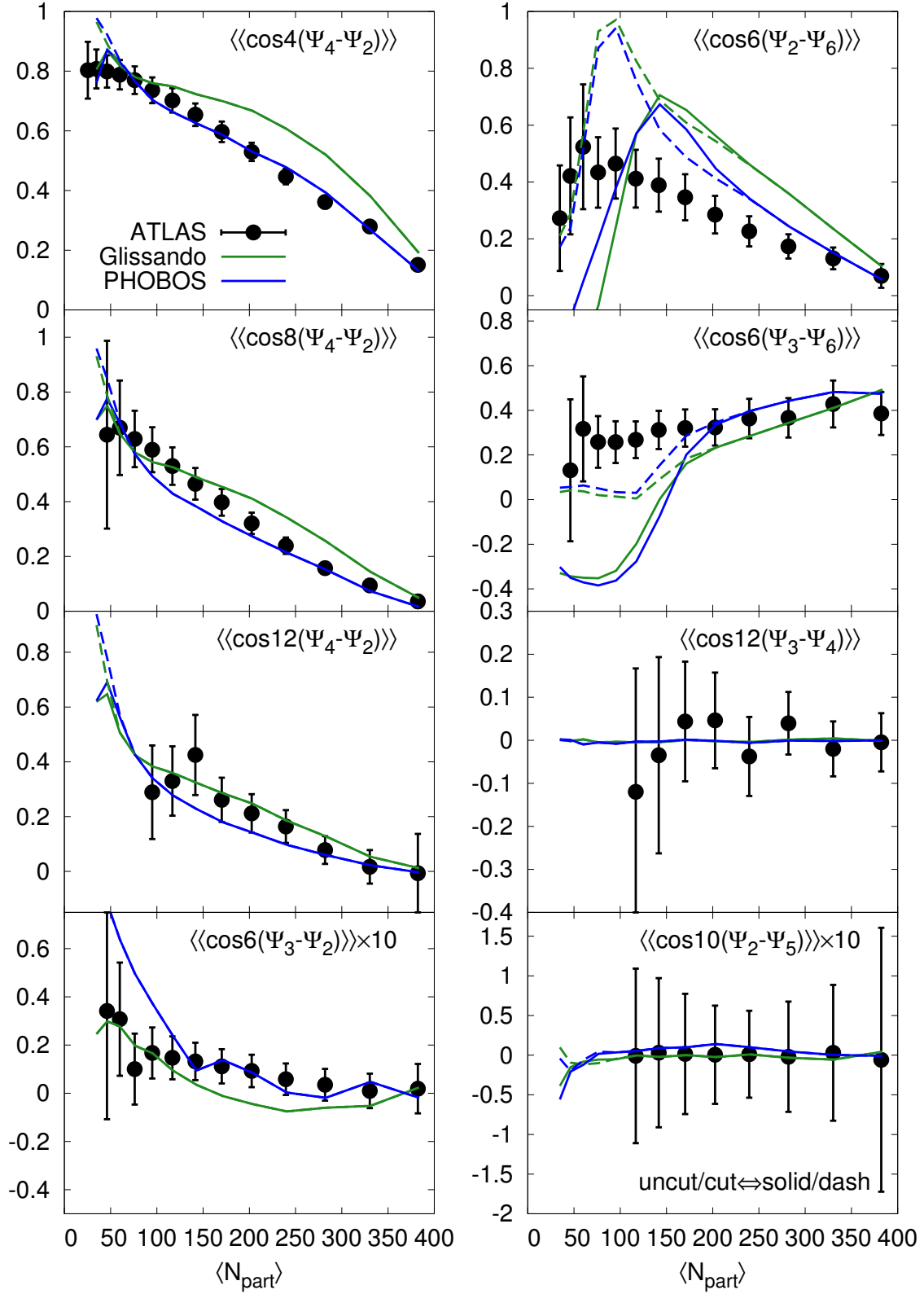


FIG. 5. (Color online) A comparison of the two-plane correlations in the high resolution limit for two different Glauber models, Glissando [15] and the PHOBOS Glauber [16]. The solid lines (un-cut) include the negative response in peripheral collisions due to a large δf , while the dashed lines (cut) truncate the negative response – see Section III.

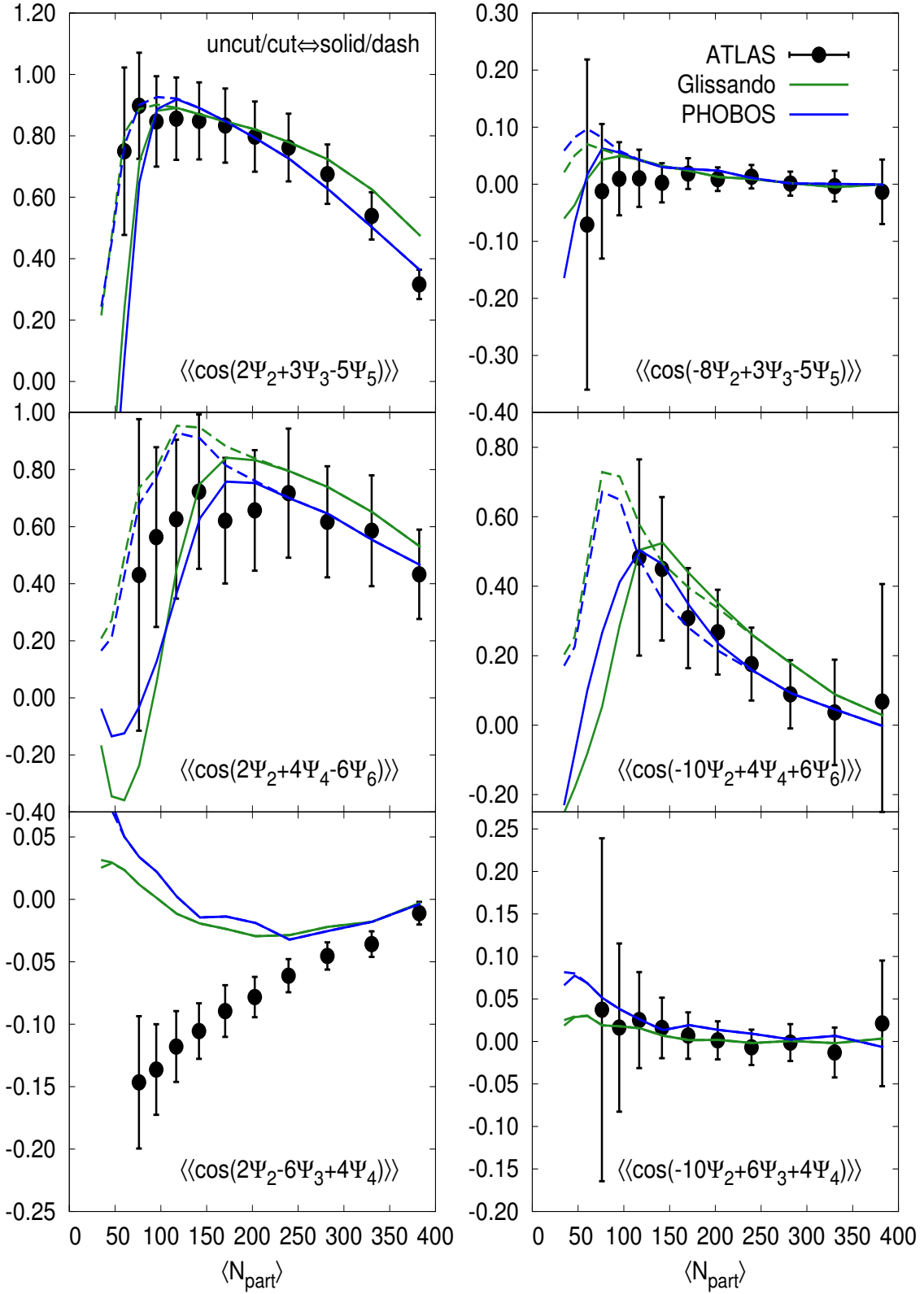


FIG. 6. (Color online) A comparison of the three-plane correlations in the high resolution limit for two different Glauber models, Glissando [15] and the PHOBOS Glauber [16]. The solid lines (un-cut) include the negative response in peripheral collisions due to a large δf , while the dashed lines (cut) truncate the negative response – see Section III.

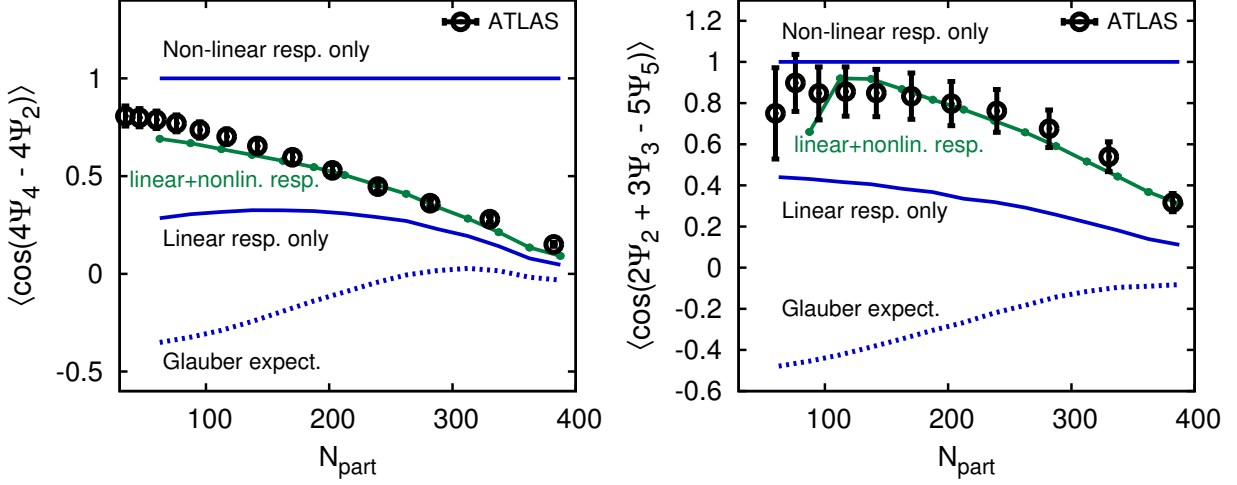


FIG. 7. The separate contributions of the linear and non-linear response to a two-plane correlation, $\langle \cos(4\Psi_4 - 4\Psi_2) \rangle$, and a three-plane correlation, $\langle \cos(2\Psi_2 + 3\Psi_3 - 5\Psi_5) \rangle$. The dashed lines show the naive Glauber expectation (see text). The data is from Ref. [9].

v_4 with v_3 . Indeed, a preliminary analysis suggests that this correlation is closely related to the transverse shift from the geometrical center to the center of participants. The 2, 3, 4 correlation is qualitatively reproduced by event-by-event hydrodynamics [12].

It is important and instructive to understand the hydrodynamic origin of the correlations presented in these figures. This is best understood by examining the linear and non-linear contributions separately. Fig. 7(a) and (b) illustrate this decomposition with the correlations $\langle \cos(4(\Psi_2 - \Psi_4)) \rangle$ and $\langle \cos(2\Psi_2 + 3\Psi_3 - 5\Psi_5) \rangle$ respectively. For definiteness, we study the 2,3,5 combination shown in Fig. 7(b). The naive expectation of the Glauber model (where v_n is proportional to the n -th order moment based eccentricity) is shown by the dotted line, and has the wrong sign. In the naive approach the observed correlation between the event plane angles 2, 3, 5 arises from the correlations between the angles associated with the corresponding moment based eccentricities.

In the current work the v_5 is produced through a combination of the linear and non-linear response.

- In linear response, v_5 is proportional to the 5-th cumulant ϵ_5 , and the correlation between the event plane angles Ψ_2, Ψ_3, Ψ_5 reflects the initial state correlation between the associated cumulant angles, Φ_2, Φ_3, Φ_5 . The predictions of linear response are shown in Fig. 7, and fail to reproduce the observed correlations in non-central collisions.
- In non-linear response, v_5 is determined through the mode mixing of v_2 and v_3 . If v_5 was determined entirely by this mechanism, the Ψ_5 event plane would be entirely determined by Ψ_2 and Ψ_3 , leading to a perfect 2, 3, 5 correlation. This prediction of non-linear response is also shown in Fig. 7.

In general, v_5 is determined by a weighted average of the linear and non-linear response curves. The relative size of these two contributions is determined by viscous hydrodynamics which predicts the magnitude of these response coefficients as a function of centrality. Evidently, hydrodynamics and the response formalism reproduces the centrality dependence of

the observed correlation functions. It is satisfying to see how the data transition between the linear response curves in central collisions, and the non-linear response curves in peripheral collisions.

Finally, we conclude by discussing the importance of higher order terms in the response formalism. First, we have neglected the third order mixing of harmonics. The most important third order term is proportional to \mathcal{E}_2^3 , and we have found that this term is small compared to the \mathcal{E}_3^2 and $\mathcal{E}_2\mathcal{E}_4$ terms. Thus, the response formalism seems to converge, and including the mixing of higher harmonics will not change the results of this study significantly.

In the future it will be important to characterize the fluctuations around the response formalism. For any given initial state characterized by a few macroscopic cumulants such as $\mathcal{E}_2, \mathcal{E}_3, \mathcal{E}_4 \dots$, the observed v_n will on *average* be given by the response formalism. However, additional fluctuations (which leave the macroscopic cumulants fixed) will reduce the perfect correlation between v_2, v_3, v_4, \dots and the predictions of non-linear response. Thus, in general, the response formalism will overestimate the strength of the correlations that are observed. Ideally, the fluctuations around the response formalism can be parametrized by universal Gaussian noise, which will be independent of the microscopic details of the initial state. The study of fluctuations around the response formalism is left for future work.

Acknowledgments:

We thank J. Y. Ollitrault, Z. Qiu, U. Heinz, J. Jia, and S. Mohapatra for many constructive and insightful comments. D. Teaney is a RIKEN-RBRC fellow. This work is supported by the Department of Energy, DE-FG-02-08ER4154.

-
- [1] Ulrich W Heinz and Raimond Snellings, “Collective flow and viscosity in relativistic heavy-ion collisions,” (2013), [arXiv:1301.2826 \[nucl-th\]](#).
 - [2] Boris Hippolyte and Dirk H. Rischke, “Global variables and correlations: Summary of the results presented at the Quark Matter 2012 conference,” [Nucl.Phys. **A904-905**, 318c–325c \(2013\)](#), [arXiv:1211.6714 \[nucl-ex\]](#).
 - [3] Derek A. Teaney, “Viscous Hydrodynamics and the Quark Gluon Plasma,” (2009), invited review for ‘Quark Gluon Plasma 4’. Editors: R.C. Hwa and X.N. Wang, World Scientific, Singapore., [arXiv:0905.2433 \[nucl-th\]](#).
 - [4] B. Alver and G. Roland, “Collision geometry fluctuations and triangular flow in heavy-ion collisions,” [Phys.Rev. **C81**, 054905 \(2010\)](#), [arXiv:1003.0194 \[nucl-th\]](#).
 - [5] Zhi Qiu and Ulrich W. Heinz, “Event-by-event shape and flow fluctuations of relativistic heavy-ion collision fireballs,” [Phys.Rev. **C84**, 024911 \(2011\)](#), [arXiv:1104.0650 \[nucl-th\]](#).
 - [6] Fernando G. Gardim, Frederique Grassi, Matthew Luzum, and Jean-Yves Ollitrault, “Mapping the hydrodynamic response to the initial geometry in heavy-ion collisions,” [Phys.Rev. **C85**, 024908 \(2012\)](#), [arXiv:1111.6538 \[nucl-th\]](#).

- [7] Nicolas Borghini and Jean-Yves Ollitrault, “Momentum spectra, anisotropic flow, and ideal fluids,” *Phys.Lett.* **B642**, 227–231 (2006), [arXiv:nucl-th/0506045 \[nucl-th\]](#).
- [8] Derek Teaney and Li Yan, “Non linearities in the harmonic spectrum of heavy ion collisions with ideal and viscous hydrodynamics,” *Phys.Rev.* **C86**, 044908 (2012), [arXiv:1206.1905 \[nucl-th\]](#).
- [9] The ATLAS Collaboration, “Measurement of reaction plane correlations in Pb-Pb collisions at $\sqrt{s_{NN}}=2.76$ TeV,” (May, 2012), ATLAS-CONF-2012-049. See also <https://cdsweb.cern.ch/record/1451882>.
- [10] Ante Bilandzic (ALICE Collaboration), “Anisotropic flow measured from multi-particle azimuthal correlations for Pb-Pb collisions at 2.76 TeV by ALICE at the LHC,” *Nucl.Phys.A904-905* **2013**, 515c–518c (2013), [arXiv:1210.6222 \[nucl-ex\]](#).
- [11] Matthew Luzum and Jean-Yves Ollitrault, “The event-plane method is obsolete,” *Phys.Rev.* **C87**, 044907 (2013), [arXiv:1209.2323 \[nucl-ex\]](#).
- [12] Zhi Qiu and Ulrich Heinz, “Hydrodynamic event-plane correlations in Pb+Pb collisions at $\sqrt{s} = 2.76$ ATeV,” *Phys.Lett.* **B717**, 261–265 (2012), [arXiv:1208.1200 \[nucl-th\]](#).
- [13] Rajeev S. Bhalerao, Jean-Yves Ollitrault, and Subrata Pal, “Event-plane correlators,” (2013), [arXiv:1307.0980 \[nucl-th\]](#).
- [14] Charles Gale, Sangyong Jeon, Bjorn Schenke, Prithwish Tribedy, and Raju Venugopalan, “Event-by-event anisotropic flow in heavy-ion collisions from combined Yang-Mills and viscous fluid dynamics,” *Phys.Rev.Lett.* **110**, 012302 (2013), [arXiv:1209.6330 \[nucl-th\]](#).
- [15] Wojciech Broniowski, Maciej Rybczynski, and Piotr Bozek, “GLISSANDO: Glauber initial-state simulation and more..” *Comput.Phys.Commun.* **180**, 69–83 (2009), [arXiv:0710.5731 \[nucl-th\]](#).
- [16] B. Alver, M. Baker, C. Loizides, and P. Steinberg, “The PHOBOS Glauber Monte Carlo,” (2008), [arXiv:0805.4411 \[nucl-ex\]](#).
- [17] Stefan Floerchinger and Urs Achim Wiedemann, “Mode-by-mode fluid dynamics for relativistic heavy ion collisions,” (2013), [arXiv:1307.3453](#).
- [18] Stefan Floerchinger and Urs Achim Wiedemann, “Kinetic freeze-out, particle spectra and harmonic flow coefficients from mode-by-mode hydrodynamics,” (2013), [arXiv:1311.7613 \[hep-ph\]](#).
- [19] Li Yan, “A Hydrodynamic Analysis of Collective Flow in Heavy-Ion Collisions,” Ph.D. thesis, Stony Brook University (2013).
- [20] Kevin Dusling, Guy D. Moore, and Derek Teaney, “Radiative energy loss and $v(2)$ spectra for viscous hydrodynamics,” *Phys.Rev.* **C81**, 034907 (2010), [arXiv:0909.0754 \[nucl-th\]](#).
- [21] Mikko Laine and York Schroder, “Quark mass thresholds in QCD thermodynamics,” *Phys.Rev.* **D73**, 085009 (2006), [arXiv:hep-ph/0603048 \[hep-ph\]](#).

- [22] Matthew Luzum and Paul Romatschke, “Conformal Relativistic Viscous Hydrodynamics: Applications to RHIC results at $\sqrt{s} = 200$ GeV,” *Phys. Rev.* **C78**, 034915 (2008), [arXiv:0804.4015 \[nucl-th\]](#).
- [23] Derek Teaney and Li Yan, “Second order viscous corrections to the harmonic spectrum in heavy ion collisions,” (2013), [arXiv:1304.3753 \[nucl-th\]](#).
- [24] Rajeev S. Bhalerao, Matthew Luzum, and Jean-Yves Ollitrault, “Understanding anisotropy generated by fluctuations in heavy-ion collisions,” *Phys.Rev.* **C84**, 054901 (2011), [arXiv:1107.5485 \[nucl-th\]](#).
- [25] Rajeev S. Bhalerao, Matthew Luzum, and Jean-Yves Ollitrault, “Determining initial-state fluctuations from flow measurements in heavy-ion collisions,” *Phys.Rev.* **C84**, 034910 (2011), [arXiv:1104.4740 \[nucl-th\]](#).
- [26] Georges Aad *et al.* (ATLAS Collaboration), “Measurement of the distributions of event-by-event flow harmonics in lead–lead collisions at $\sqrt{s_{NN}}=2.76$ TeV with the ATLAS detector at the LHC,” (2013), [arXiv:1305.2942 \[hep-ex\]](#).
- [27] B. Alver *et al.* (PHOBOS Collaboration), “Event-by-Event Fluctuations of Azimuthal Particle Anisotropy in Au + Au Collisions at $\sqrt{s_{NN}} = 200$ GeV,” *Phys.Rev.Lett.* **104**, 142301 (2010), [arXiv:nucl-ex/0702036 \[nucl-ex\]](#).
- [28] Burak Han Alver, Clement Gombeaud, Matthew Luzum, and Jean-Yves Ollitrault, “Triangular flow in hydrodynamics and transport theory,” *Phys.Rev.* **C82**, 034913 (2010), [arXiv:1007.5469 \[nucl-th\]](#).